EUROPEAN SYNCHROTRON RADIATION FACILITY
INSTALLATION EUROPEENNE DE RAYONNEMENT SYNCHROTRON

ESRF

ESRF	**Experiment title:** Quantification of vessel trees from tumors down to the capillary level	**Experiment number**: MD-407
Beamline: ID19	**Date of experiment**: from: 18.06.2009 to: 25.06.2009	**Date of report**: 01.09.09
Shifts: 18	**Local contact(s)**: Timm Weitkamp	*Received at ESRF:*

Names and affiliations of applicants (* indicates experimentalists):

Bert Müller[1], Franz Pfeiffer[2,3], Christian David[3], Timm Weitkamp[4], Sabrina Lang[1]

Experimentalists at beamline:

Bert Müller[1], Christian David[3], Timm Weitkamp[4], Sabrina Lang[1], Irene Zanette[4], Georg Schulz[1], Simon Rutishauser[3]

[1]*Biomaterials Science Center, University Basel, 4031 Basel, Switzerland*

[2]*Department of Physics / Biophysics, Technical University of Munich, 85748 Garching, Germany*

[3]*Paul Scherrer Institute, 5232 Villigen PSI, Switzerland*

[4]*ID19, European Synchrotron Radiation Facility, 38042 Grenoble Cedex, France*

1. Summary

The experiment was focused on the visualization of the tumor vessel tree down to the capillaries. At the beamline ID 19 we have carried out phase contrast micro computed tomography (μCT) based on grating interferometry for seven C51 human tumors grown in nude mice. In order to optimize both spatial and density resolution, the FReLoN 2K detection unit with a pixel size of 5.06 μm was chosen. To analyze the potential influence of tissue fixation, the specimens were stored and measured in three different solutions.
In addendum to experiment MD-328 we imaged two parts of human brain containing the thalamus and a part of the cerebellum.

2. Visualization of the tumor vessel tree

The visualization of the tumor vascular network requires, on the one hand, a spatial resolution down to micrometer to visualize also the smallest capillaries and, on the other hand, high density resolution in order to distinguish the vessels from the surrounding tissue. To solve this task we have applied the grating interferometry μCT. Contrary to the conventional absorption mode, the grating interferometry relies on phase shift detection and is, therefore, much more sensitive for soft tissue imaging. Consequently, the tissue preparation has become rather simple, since any staining of the vessels is avoided.

2.1 Specimen preparation

For the differential phase contrast μCT experiments we prepared seven tumors by injecting C51 tumor cells of human origin into nude mice exactly one week before the planned measurements. Well in time, the mice were sacrificed to extract the tumors and to transfer them into the liquid-filled Eppendorf containers. Three of the tumors were fixed in a solution with 4% para-formaldehyd (PFA) to suppress decomposition. Two of them were immersed in phosphate buffered saline (PBS) to prevent tumor drying and shrinkage. Finally, two tumors were immersed in Alsever, an isotonic, balanced salt solution routinely used as anticoagulant/blood preservative, permitting the storage of blood at refrigerator temperatures for approximately 10 weeks [1]. The tumors, not fixed in formaldehyd after extraction, were fixed just after the tomography experiment to avoid further decomposition.

Pieces of a straw fixed the tumors inside the container to avoid relative movements during data acquisition.

2.2 Experimental set-up

In order to illuminate the tumors with different diameters for tomography at the beamline ID 19, we have selected the undulator U32d with a gap of 15.15 mm and the wiggler W150m with a gap of 80.00 mm. For data acquisition we have used a beam-splitter grating g_1 with a period of 4.785 μm and an absorption grating g_2 with a period of 2.400 μm. The distance between the gratings was adjusted to 479.3 mm to reach the 9^{th} Talbot distance at the photon energy of 23 keV. The FReLoN 2K detection unit allowed us to realize a field of view of $10.36 \times 6.07\ mm^2$ with a pixel size of 5.06 μm and $39.38 \times 13.94\ mm^2$ with a pixel size of 31.25 μm.

The specimens, hold in the Eppendorf container, were placed into a water-filled box with parallel PMMA walls to reduce the artifacts caused by the large phase shifts at the air-Eppendorf interface. To restrict the absorption of photons in the box, the distances between the parallel walls were chosen to about 15 and 40 mm, respectively.

At each projection angle (1501 steps of 0.24 degrees) four images over one period were taken (phase-stepping). The data were reconstructed directly after acquisition using the software tools developed by T. Weitkamp, O. Bunk, and F. Pfeiffer [2].

2.3 Results

First, the data of the two tumors in PBS were acquired 12 h after extraction. Here, the two tumors were placed in one Eppendorf container and measured at different height positions. Fig. 1 shows the direct comparison of one selected slice in absorption (left) and phase contrast (right). As expected, the absorption contrast differences in the tissue at the photon energy of 23 keV are weak and only allow for vague interpretations but not for any meaningful vessel tree segmentation. The image indicates that even an optimized experimental set-up for absorption contrast will not lead to a contrast as given by the grating interferometry (right image of Fig. 1). Besides fat and muscle cells, the phase contrast image features vessels in the rim of the tumor (white arrows) and, more numerous, inside the tumor. The contrast between vessels and surrounding tissue, however, seems to be too low to apply simple intensity-based segmentation tools for the vessel tree extraction. Nevertheless, the image clearly shows vessels 20 μm in diameter. Thus, the

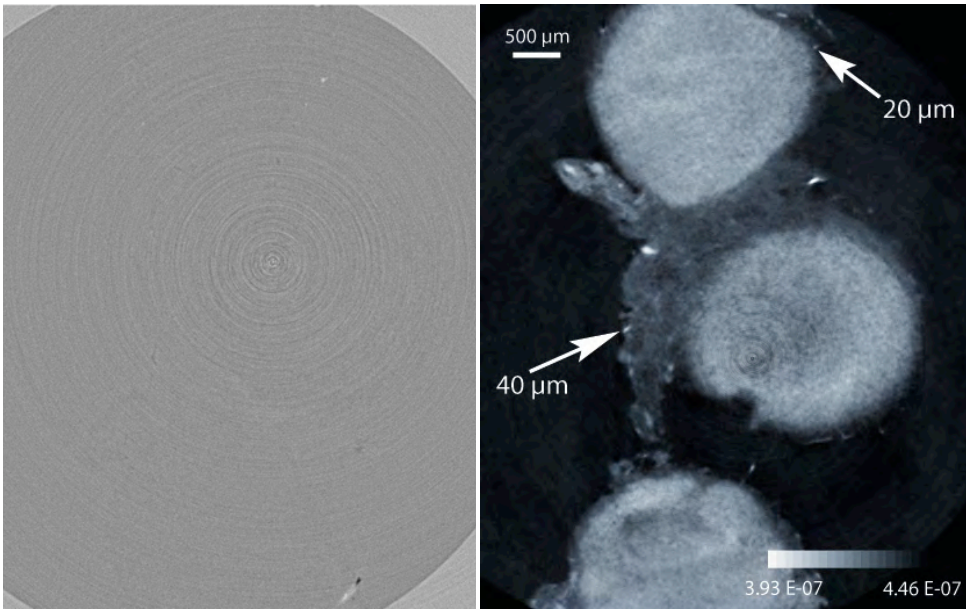

Fig. 1: *Absorption contrast image of the tumor fixed in PBS (left) and the corresponding differential phase contrast reconstruction (right). The grayscale values correspond to the decrement of the real part of the refractive index.*

application of advanced segmentation tools should permit to uncover essential parts of the vascular networks of the three C51 metastasis represented in Fig. 1.

Second, the two tumors stored in Alsever were scanned approximately 24 h after extraction. The selected images in Fig. 2 underline the results given in Fig. 1: Vessels outside the necrotic tumor are easier identified, when in the cancerous tissue and vessels with a diameter below 20 µm cannot be clearly seen. The storage of the tumors in Alsever solution leads to somehow better absorption contrast images with respect to the storage in PBS as best seen for the fat cells (a). Nevertheless, the characteristic features – fat cells, muscles (b), 50 µm-wide artery (c), capsule (d) and 20 µm-wide blood vessel (e) – are much better represented in the related phase-contrast slice (Fig. 2, right).

Third, the tumors, formalin-fixed immediately after extraction, were imaged. In absorption, one only recognizes the inhomogeneous tissue as whole together with the ring artifacts (see Fig. 3, left). The morphological features remain vague. In the phase contrast mode, however, one finds many well-separated details: typical arterial wall (a), 45 µm-wide vessel (b) and 20 µm-wide vessel (c). Another tumor yields a better overview (Fig. 4): an artery with an inner diameter of 50 µm (a), a 175 µm-wide vein (b), fat cell (c),

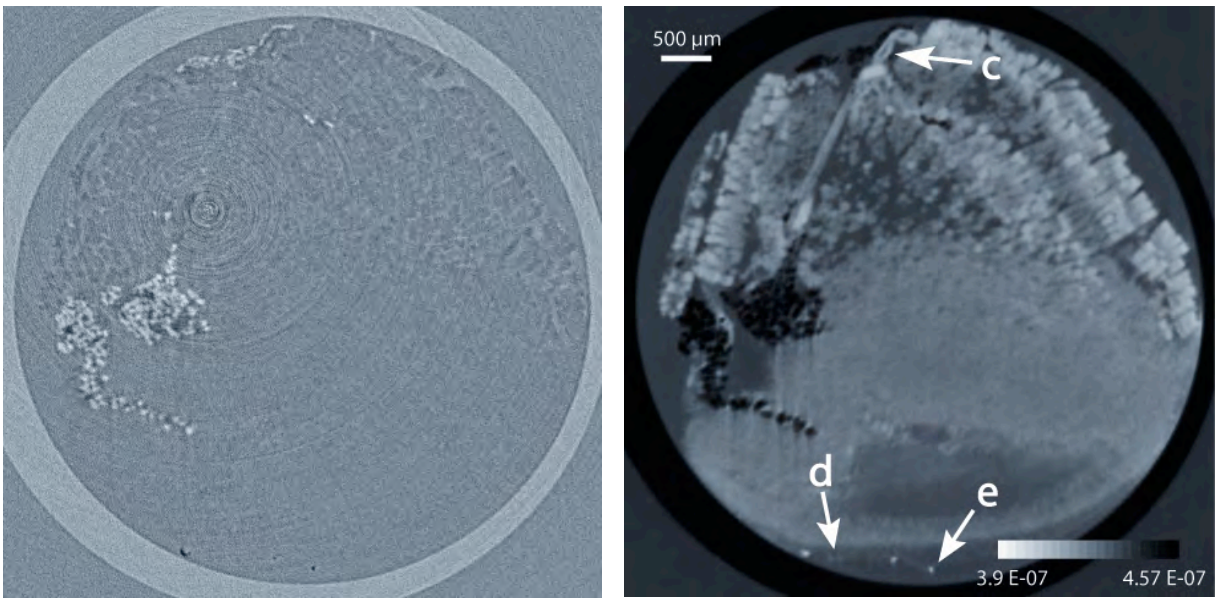

Fig. 2: *Absorption (left) and phase contrast (right) images of a tumor in Alsever.*

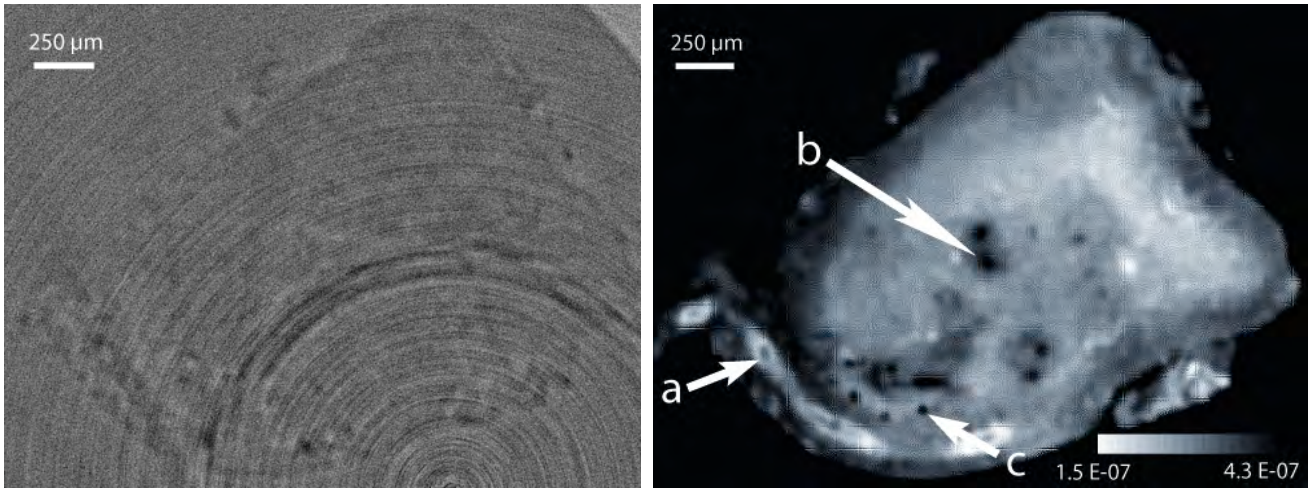

Fig. 3: *4% PFA-fixed tumor in absorption (left) and phase (right) contrast mode.*

the necrotic tumor part (d) and muscle (f). Some elements, however, cannot be uniquely associated with tissue components. For example the feature (e) could be a vessel or muscle string. For discrimination, conventional histology is required. The contrast in the tomograms of the PFA-fixed tumors is better than that of the PBS- and Alsever-fixed ones. Therefore, we have again imaged the PBS-fixed tumor (shown in Fig. 1) after 48 h PFA-fixation. Fig. 5 shows a selected tomography slice in absorption and phase contrast. While the fat cells (b) are prominent features in both slices, the phase contrast image uncovers blood vessels as an artery with an inner diameter of 50 µm. The comparison of Figs. 1 and 5 indicates that formalin fixation significantly enhances the contrast.

2.4 Outlook

Since the tomography data are not forwardly interpreted, we plan conventional histology of selected tumor parts. Together this information, the blood vessel system will be segmented. The segmented data will be quantified in order to directly compare them with simulations on the tumor formation and growth. The results will be also registered with the less detailed in-vivo data (PET and MRI) to obtain a comprehensive overview of the processes in the tumor formation and growth. Together with our partners at the ETH Zürich we are going to develop strategies again cancer, once the results are fully analyzed.

Unfortunately the resolution allowed only the identification of vessels down to 20 µm, although the smallest vessels are known to be between 2 and 4 µm in diameter. Therefore, we are looking for improved spatial resolution in grating interferometry and for alternative approaches such as holotomography.

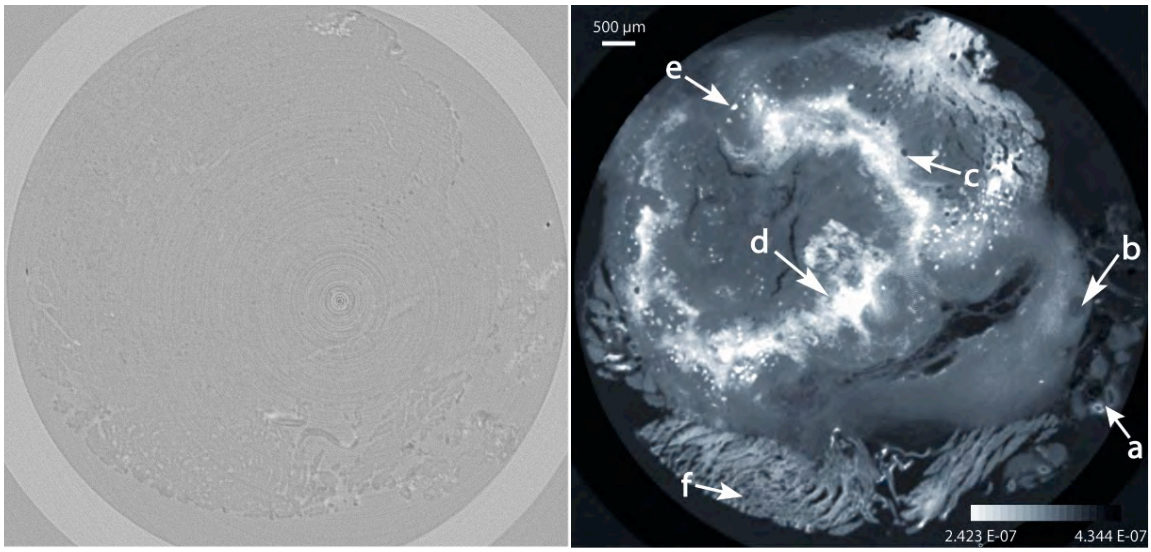

Fig. 4: *Another tumor fixed in PFA using absorption (left) and phase (right) contrast tomography.*

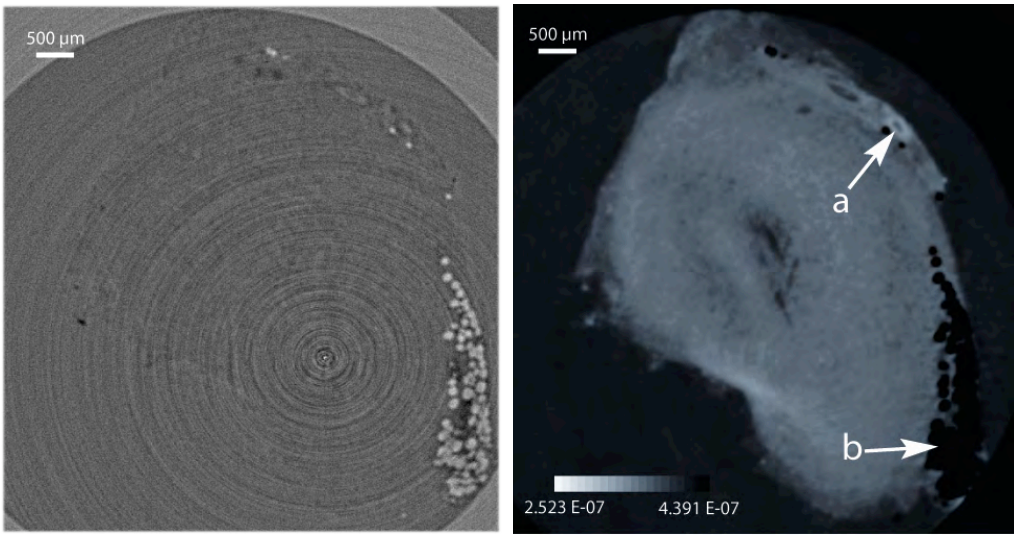

Fig. 5: *Identical tumor as in Fig. 1 after 48 h in PFA in absorption (left) and phase contrast (right) mode.*

3. Grating interferometry of human brain

MR-guided neurosurgery without intracerebral penetration using e.g. high-intensity focused ultrasound is a completely non-invasive technique. This technique requires a detailed knowledge of the morphology of the brain with a resolution down to the micrometer level. So far histological slices are used to construct such a brain atlas (e.g. [3]). These brain atlases achieve the needed spatial resolution down to sub-micrometer level laterally but also have some imperfections like shrinkage during fixation in formalin or local deformations caused by the mechanical sectioning of the brain blocks [4]. The aim of the project lies in the non-destructive visualization to correct the imperfections of the histological slices. Although MR imaging affords the required density resolution featuring a contrast between white and gray matter, it does not have the needed micrometer resolution. Using conventional absorption contrast micro computed tomography we get the spatial micrometer resolution but hardly contrast between white and gray matter. Phase contrast micro computed tomography should offer both spatial resolution down to micrometer level and the required density resolution to image varieties inside the internal structure.

3.1 Specimen preparation

In this experiment we imaged two parts of human brain: cerebellum and thalamus. The preparation of the human brain specimens proceeded as follows. After the extraction of the brain from the cranium it was fixed in 10% formalin for about 2 months. The block preparation was then carried out by A. Morel (University Hospital Zurich). The resulted dimension of the cerebellum block was 6×6×11 mm^3 and that of the thalamus block 30×30×35 mm^3. After sectioning, the blocks were placed in 4% formalin, where they also were located during the measurements.

3.2 Results

A. Cerebellum

The dimension of the cerebellum block allowed us to use the pixel size of 5.06 µm. For this scan we used the same adjustments as for the experiments imaging the tumors. In order to image the whole block, scans of two different heights were combined.

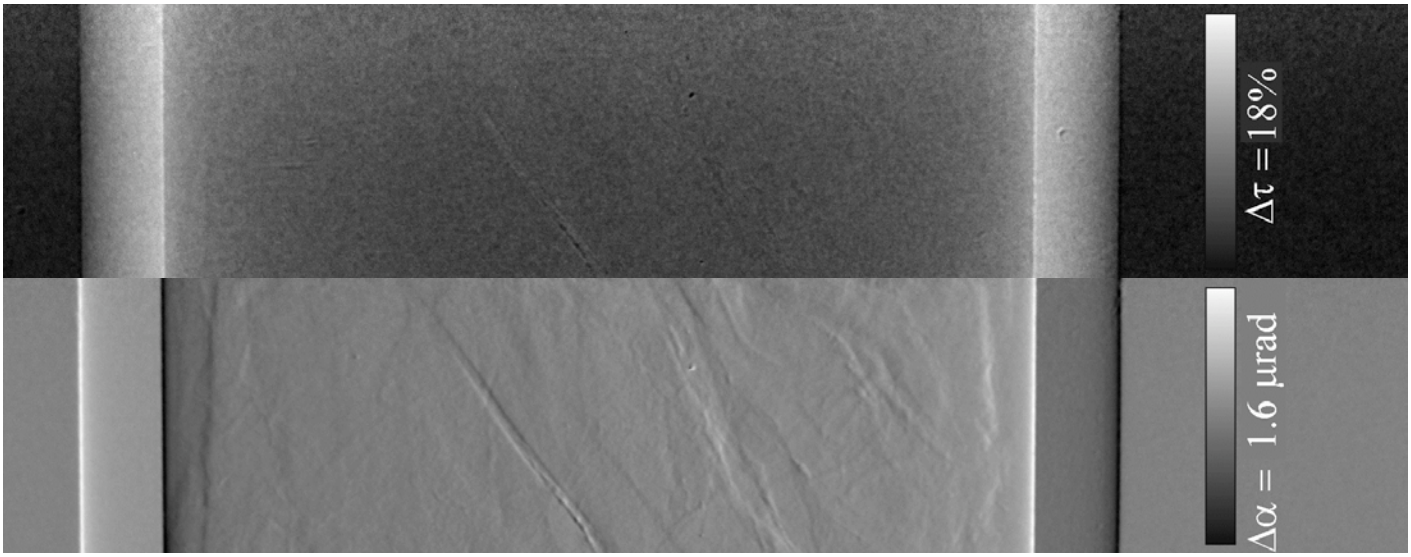

***Fig. 6**: Transmission τ (top) and deflection angle α (bottom) images of one projection angle.*

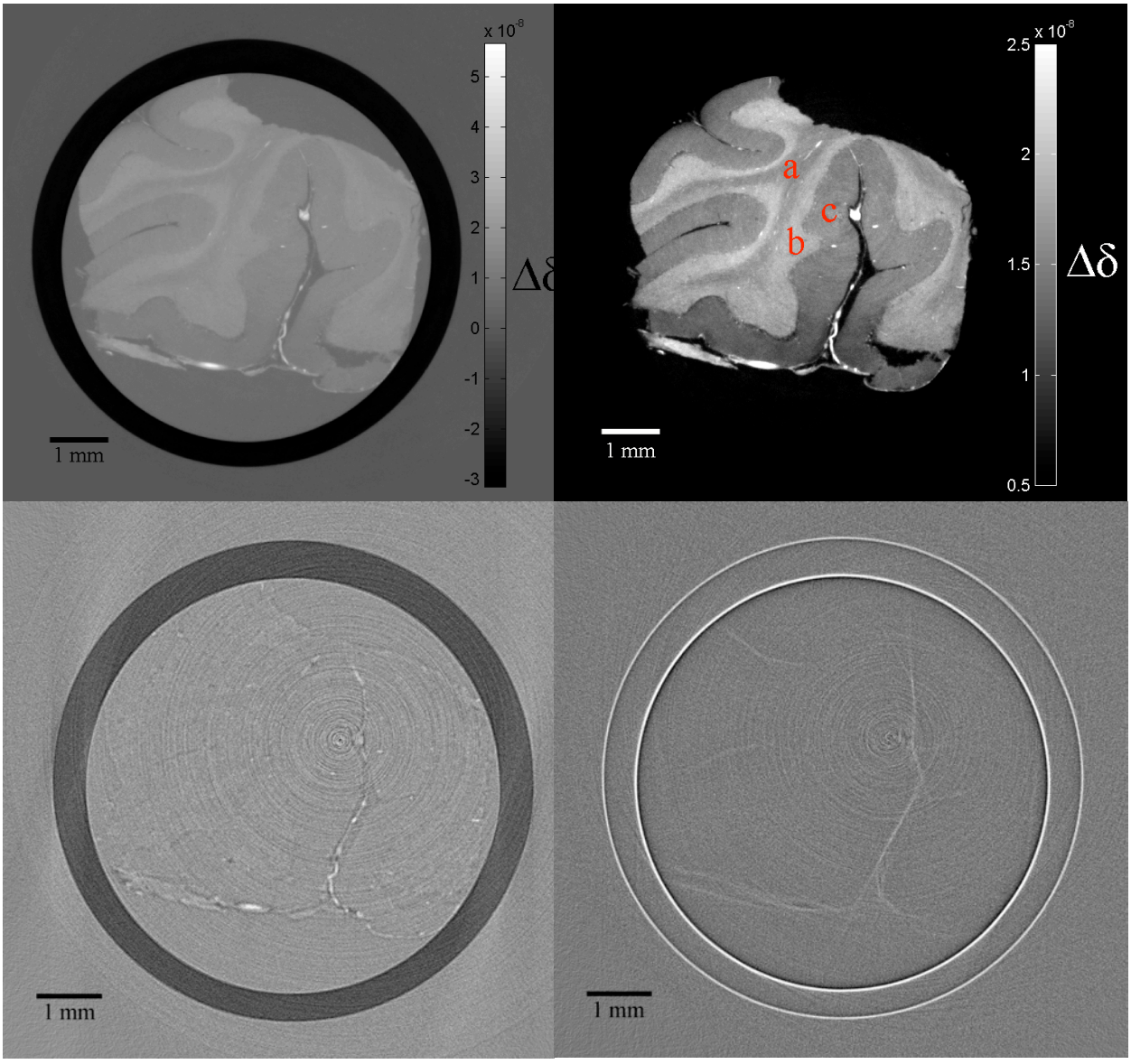

***Fig. 7:** Phase contrast (top), absorption contrast (bottom left) and dark field (bottom right) reconstructions. The upper two images show the decrement of the real part of the refractive index relatively to water Δδ for two different grayscale ranges.*

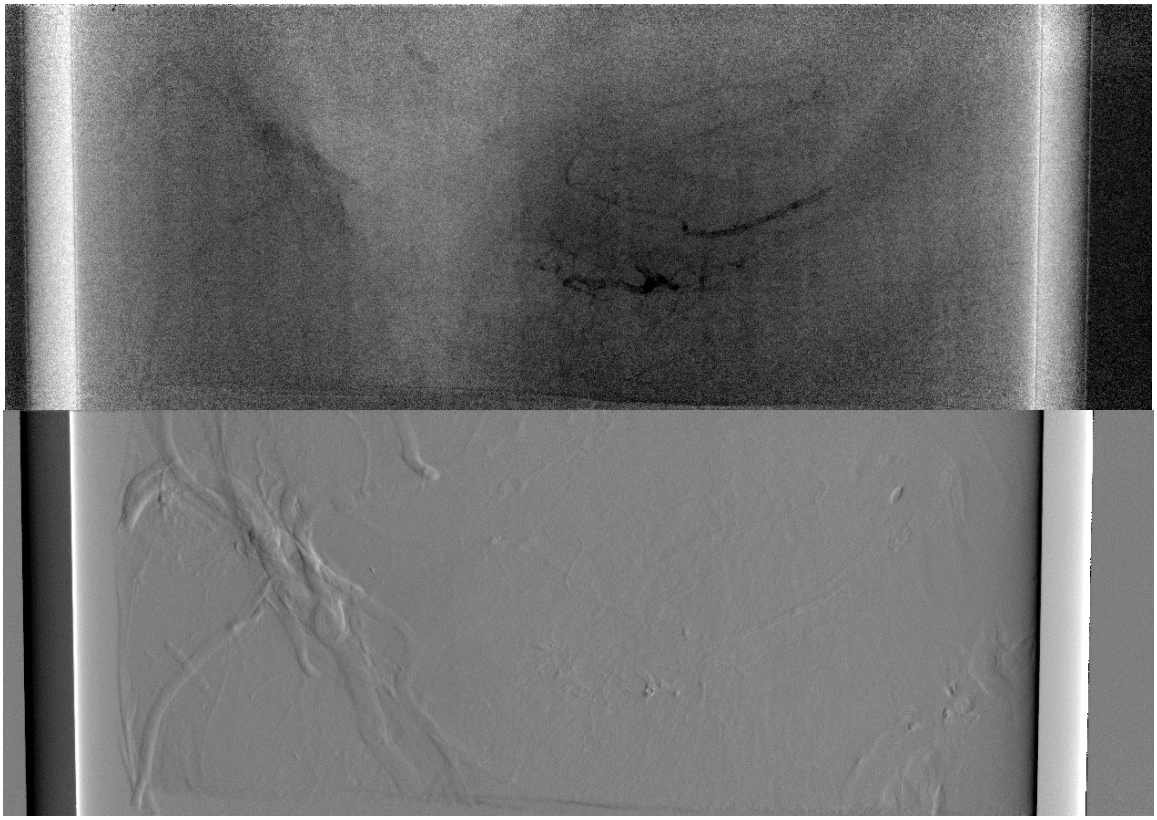

Fig. 8: *The transmission difference (top) through the thalamus in the selected projection image has the value $\Delta\tau$=11% whereas the deflection angles range lies between -0.8 and 0.8 μrad.*

Fig. 6 shows a transmission image compared to the corresponding deflection angle image. The deflection angles range is between -0.795 and 0.780 μrad. Whereas the transmission projection image only vaguely shows that it concerns the corresponding projection of the same sample (see streak in the middle of the sample), one can already discover some structures inside the sample in the deflection angle projection image. As expected, the reconstructed slices in Fig. 7 feature more information about the sample. Whereas one can only detect the boarders of the sample in the dark field image (bottom right) and additionally really dimly some structures in the absorption contrast image (bottom left), a bright contrast between the *medulla* (a) (according to white matter) and the *cortex* (b, c) (according to grey matter) of the cerebellum can be presented in the phase contrast images (top). Additionally one can differentiate between the *stratum granulosum* (b) mainly consisting of nerve and glial cells and the *stratum moleculare* (c) only including a small number of cells relatively to the *stratum granulosum*. Between the *stratum granulosum* and the *stratum moleculare* a third stratum is expected, the so-called *stratum gangliosum* composed of large *Purkinje* cells. More information about the composition of human cerebellum can be found in specialized textbooks [5, 6]. It has to be mentioned that the photon energy was too high to obtain optimal absorption contrast results.

B. Thalamus

For the scan of the thalamic block we used the pixel size of 31.25 μm. The imaging of the whole block was then partitioned in four scanning heights.

Fig. 8 contains a transmission image of one selected projection angle and the corresponding deflection angle image. On the right side of the transmission image we can see some dark structures having the shape of thin blood vessels what one can only hardly detect in the deflection angle projection. On the other hand one can clearly see bigger blood vessels in the deflection angle image (left side), which has quite no contrast in the transmission image.

Fig. 9 right shows a reconstruction of the dark field projections. Akin to the dark field images of the cerebellum these reconstructions feature the boarders between different structures and materials. Of course the high absorbing material is also clearly visible in the reconstruction of the absorption contrast projections shown in Fig. 9 left. The identification of this material will follow through the analysis of the histological slices of this object. Beside the high absorbing structures the absorption contrast images vaguely feature the contour of the thalamus and some bigger blood vessels absorbing less than the white structure in the middle. More interesting is the dark structure inside the thalamus having the shape of a 'Y'. This structure cannot be clearly identified in the corresponding differential phase contrast reconstruction shown in Fig. 10 (the borderline is not well-defined in the two images). These images show bright contrast between the thalamus and the formalin as well as between the blood vessels and the surrounding tissue. Furthermore one can differentiate between other structures (grey / white matter) inside the sample, which will be identified after the analysis of the corresponding histological slices.

Even though the differential phase contrast images show the best results the question exists whether a combination of both absorption contrast (having additional information of the interior structure) and differential phase contrast reconstructions, would afford the best result for the comparison and registration with the histological slices.

3.3 Outlook

The next step of this project is the sectioning and staining of the two specimens. The result will be two sets of histological slices, which can be digitalized using an optical microscope. On the one hand, these data-sets will help us to identify the structures shown in the tomographic reconstructions, on the other hand, we will be able to calculate the deformation field (caused by sectioning the histological slices) using three dimensional non-rigid registration of the differential phase contrast data-sets with the according histological data-sets and so to improve the brain atlas.

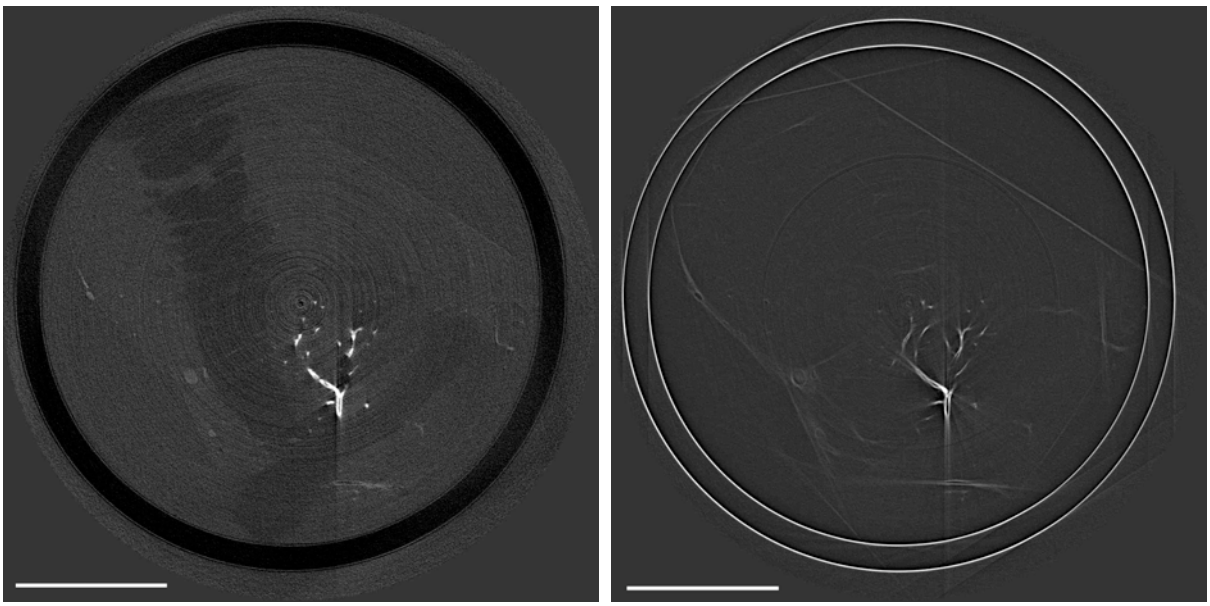

Fig. 9: *Absorption contrast (left) and dark field (right) reconstructions of the thalamus with a bar of 1 cm.*

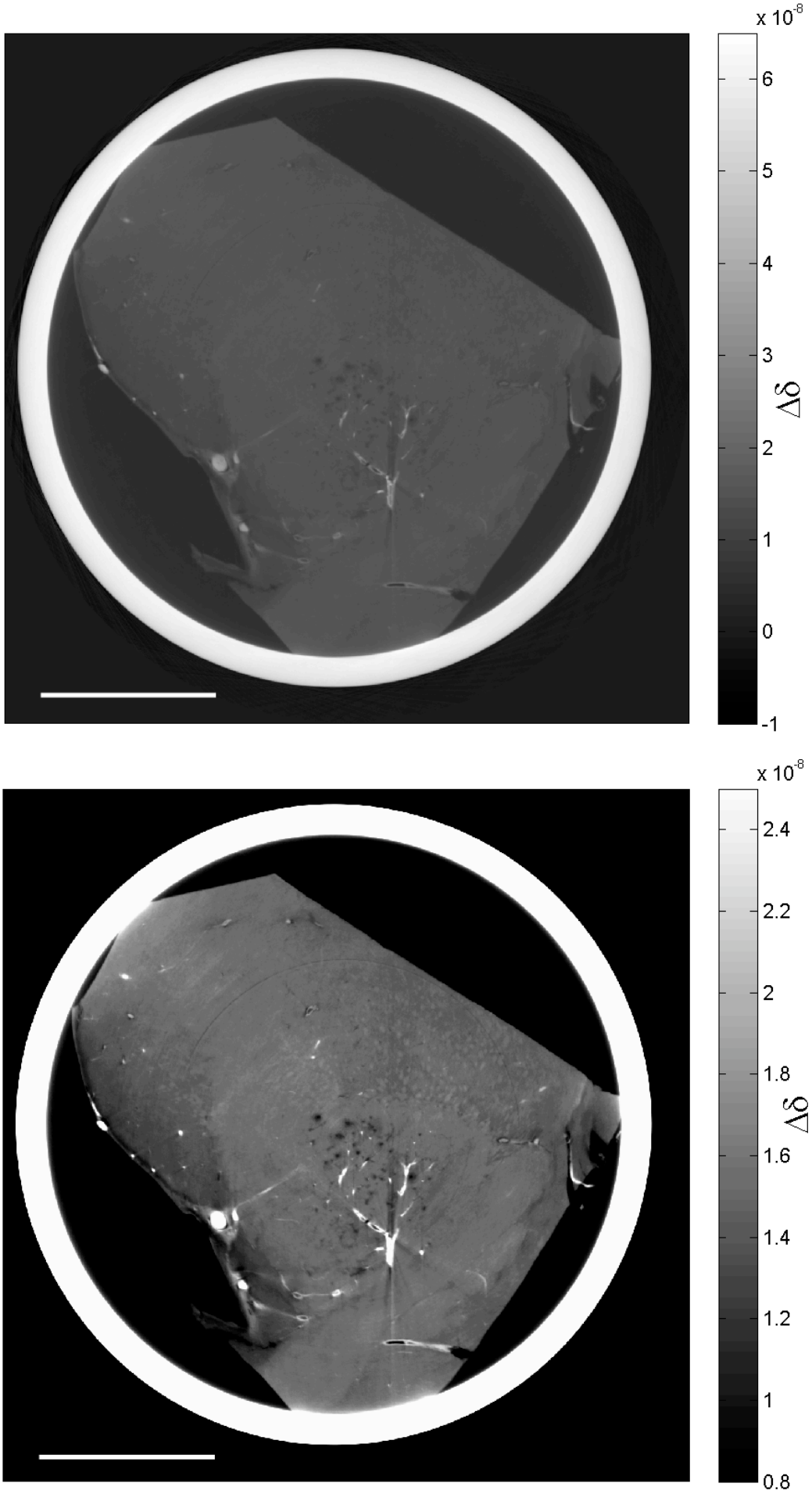

Fig. 10: *Phase contrast reconstruction showing the same slice with two different grey scale ranges. The bar equates to 1cm.*

References

[1]: J. B. Alsever, R. W. Ainslie, “A new method for the preparation of dilute blood plasma and the operation of a complete transfusion service,” J. Med. **41**, 126-131 (1941).

[2]: F. Pfeiffer, O. Bunk, C. Kottler, and C. David, "Tomographic reconstruction of three-dimensional objects from hard X-ray differential phase contrast projection images," Nucl. Instrum. Methods Phys. Res., Sect. **A 580**, 925-928 (2007).

[3]: A. Morel, “Stereotactic atlas of the human thalamus and basal ganglia,” New York, Informa Healthcare (2007).

[4]: M. Germann, A. Morel, F. Beckmann, A. Andronache, D. Jeanmonod, and B. Müller, “Strain fields in histological slices of brain tissue determined by synchrotron radiation-based micro computed tomography,” J. Neurosci. Methods **170**, 149-155 (2008).

[5]: Sobotta / Hammersen, “Histologie Farbatlas der Mikroskopischen Anatomie,” 4. Auflage Urban & Schwarzenberg München-Wien-Baltimore (1994).

[6]: M. Trepel, “Neuroanatomie Struktur und Funktion,” 4. Auflage Urban & Fischer München-Jena (2008).